EFFECT OF COMPLIANCE AND BACKLASH ON THE OUTPUT SPEED OF A TRANSMISSION SYSTEM

by

R. V. Ramamurthy and P. Pagilla
Oklahoma State University
USA

ABSTRACT

Backlash is one of the most commonly encountered nonlinearities in drive systems employing gears or ball-screws and indicates the play between adjacent movable parts. Presence of backlash causes delays and oscillations and consequently gives rise to inaccuracies in the position and velocity of the machine. Coupled with this, if the drive system consists of compliant members, torsional oscillations may also occur. Though the presence of backlash may not be of utmost significance in the case of a general speed controlled drive system, web handling systems stand as a unique exception to this observation; any small change in the web speed causes large changes in the controlled tension and hence tight control of speed is an essential requirement in web handling systems. Also, it is of interest to know an estimate of the accuracy of speed achievable in a given closed-loop control system. This paper addresses the effects of compliance and backlash on the output speed of the transmission system.

A model to include the effects of compliance and backlash is proposed under the assumption that the collisions due to backlash are sufficiently plastic to avoid bouncing. The proposed model considers the compliance (which may be either due to the elasticity of the shafts or belt in a belt-pulley transmission system) and backlash appearing in series in a drive system. In contrast to the classical backlash model which considers both input and output to the backlash as displacements, the proposed model considers (torque) force as input to the backlash and (angular velocity) velocity of the driven member as the output of the backlash. Thus, the proposed model does not assume that the load is stationary when contact is lost due to backlash width, i.e., momentum of the load is taken into account in the proposed model.

From the proposed model, a bound on the speed error due to the presence of backlash is derived. To derive the bound on speed error due to backlash, two situations are considered: (i) closed-loop speed control system with a given backlash, and (ii) the same

closed-loop system with no backlash. The difference between the outputs of these two systems indicates the error caused by the backlash and represents the achievable accuracy of the closed-loop system. Closed-loop experiments were conducted on a rectilinear system to obtain the error caused by different backlash widths. The bound obtained from the experimental results agrees with the theoretically computed bound.

NOMENCLATURE

b_m, b_L	:	Viscous friction coefficients of the motor and the load
F_m, F_L	:	Forces on the motor and load
G_R	:	Gear ratio ($=R_{g2}/R_{g1}$)
J_m, J_L	:	Motor and load moments of inertia
k	:	Stiffness of the spring/shaft
K_b	:	Stiffness of the belt
L_s, L_{s0}	:	Lengths of spring or belt
M_m, M_L	:	Motor and load masses
R_1, R_2	:	Radii of pulleys
R_{g1}, R_{g2}	:	Pitch circle radii of gears
T_m, T_L	:	Torques on the motor and load
X_m, X_L	:	Displacements of motor and load
x_m, x_L, y	:	Deviations of displacements from reference position
α_1, α_2	:	Constants, $\alpha 1 = R_2 G_R$, $\alpha_2 = R_2/R_{g1}$
Δ	:	Half backlash gap
θ_m, θ_L, θ	:	Angular displacements

INTRODUCTION

Backlash is one of the most commonly encountered nonlinearities in drive systems employing gears or ball-screws and indicates the play between adjacent moveable parts. Since the action of two mating gears can be represented by the action of one pair of teeth, backlash is commonly represented by the schematic shown in Figure 1. When used in the context of mechanical engineering, backlash denotes two salient features as shown in Figure 2: (i) a mechanical hysteresis due to the presence of clearance (Δ), and (ii) impact phenomena between the surfaces of the masses (M_m and M_L).

In Figure 1, M_m and M_L are the masses (inertias) of the driving and driven members, x_m and x_L are the linear (angular) displacements of the driving and driven members, respectively, from a fixed reference position, and F_m and F_L are the driving and load forces (torques). It is a common practice to lump all the mass (inertia) on the driving side into one quantity, M_m, and refer to it as the "motor" and lump all the mass (inertia) on the driven side, and refer to it as the "load". The classical backlash model considers the schematic shown in Figure 1 with input to the backlash as the displacement x_m and the output of the backlash as the displacement x_L. The input-output characteristics of the backlash are represented by Figure 2. The slopes of lines GBC and FED are equal to the speed ratio of the gearing in the case of rotary systems.

The closed curve $BCDEFGB$ in Figure 2 represents mechanical hysteresis due to the presence of clearance Δ. At points B, D, and G in Figure 2, the two masses impact

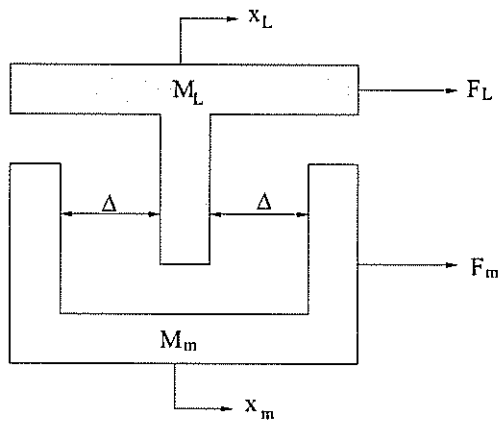

Figure 1 - Schematic of backlash

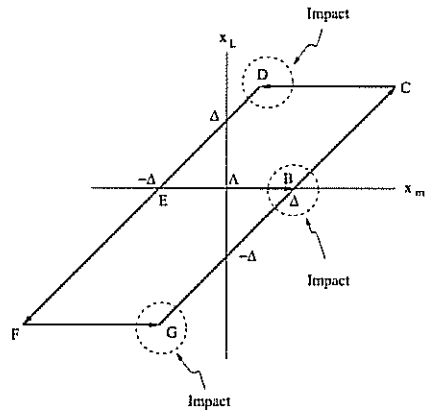

Figure 2 - Input-output plot for friction-controlled backlash

and near these points, the input-output plot may not be straight but may "oscillate" with a small amplitude. However, impact may be considered to be sufficiently plastic so that points on these lines lie along a curve bounded by the dotted circles shown, before they resume to lie on the straight lines. The classical backlash model resorts to this simplification mainly because in large industrial machines, which operate at steady state and do not reverse direction, impact does not arise except during starting/stopping conditions. Also, in smaller machines, the gear and impact energy are very small. Thus, a plastic impact is considered to be a reasonable assumption. Consequently, all the impacts are assumed to be plastic in this paper. Since large industrial machines do not reverse direction many times during their operation, the lines *CDE* and *FGB* in Figure 2 are ignored. And this prompted many researchers to erroneously consider the input-output graph of backlash to be represented by the curve *FEABC*, which is the input-output graph for dead-zone nonlinearity. Also, it may be observed that the the backlash characteristics shown in Figure 2 consider the input to the backlash to be the displacement of motor (x_m

in Figure 1) and output of the backlash to be the displacement of the load (x_L in Figure 1). However, in actual practice, the input is a force (torque) on the motor and the output is either the displacement or the velocity of the load. In such situations, the plot between x_m and x_L drastically different from that shown in Figure 2 and depends on the nature of the force applied. For example, if a force as shown in Figure 3 is applied on the motor ($M_m = 5$ kg, $M_L = 10$ kg, $b_m = b_L = 0.5$ N-s/m) in Figure 1, the plot between x_m and x_L may be obtained as shown in Figure 4. Thus, the describing function approaches based on the input-output plot shown in Figure 2 are not applicable for this case.

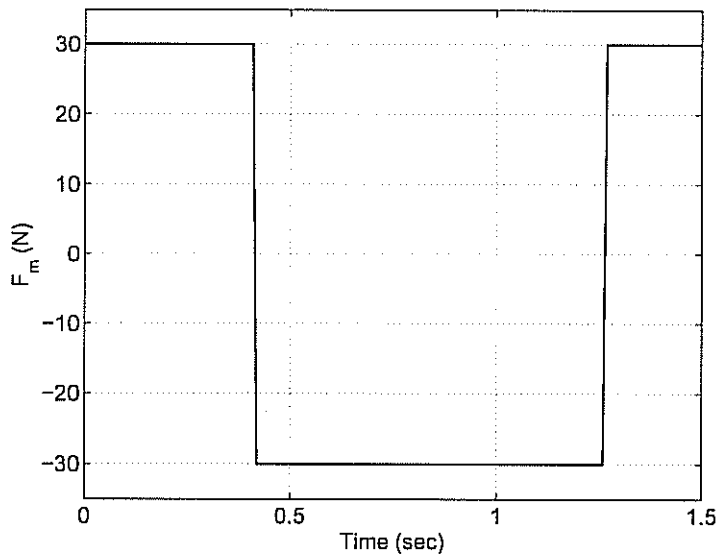

Figure 3 - Force on the motor.

Research on modeling backlash and its effects dates back to the 1960's. Much of this research focused on the method of describing functions to investigate limit cycles and deriving stability criteria for systems containing backlash [1–4]. A rectilinear model called "impact pair" was presented in [5, 6] based on which the dynamic behavior of meshing gears was studied in [7]. As a further development, a rotary model for spur gears was developed in [8] and the contact-spring rate and a time dependent damping for a pair of standard spur gears (pressure angle = 15 or 20 degrees) was computed. The dynamic model given in [8], though rigorous and which may prove very useful for the gear manufacturers, is not amenable for application by a control engineer. Consequently, a simplified dynamic model is needed.

Using the models developed, a number of researchers investigated control strategies to compensate for the effects of backlash [9–18]. These control strategies may be grouped into two main categories: (i) strategies for controlling the displacement of the driven member, and (ii) strategies for controlling the velocity of the driven member. A comprehensive survey of various such strategies is reported in [9]

A delayed output feedback controller is proposed for a backlash-free plant in [10]

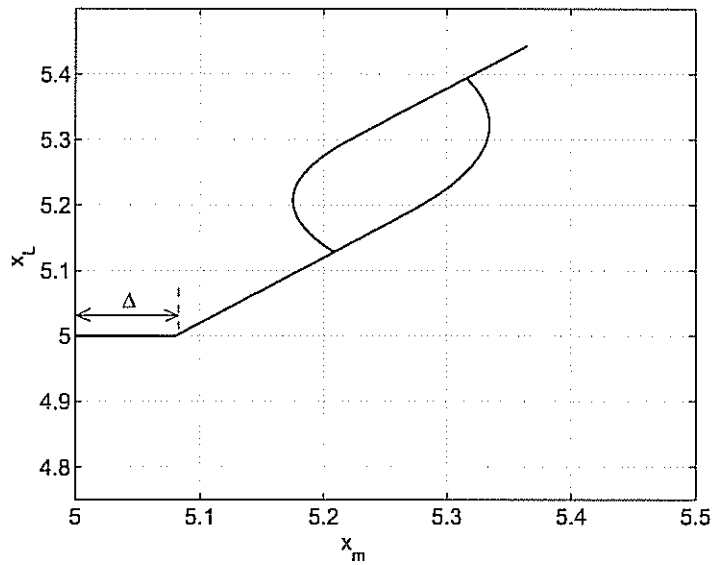

Figure 4 - Input-output plot of backlash with force as input.

to compensate for the effects of backlash with displacement as its input and output. However, it was not made clear as to how the delayed feedback controller stabilizes the system. In [11], an"adaptive right-backlash-inverse" was proposed and it was shown that all closed-loop signals are bounded. Similar work on dynamic inversion using neural networks was reported in [12, 13]. Though stability of the system using these inversion schemes is shown through simulations, it is reported in [9] that "the adaptive control seems to yield bad transients during adaptation, while after adaptation, the gain, and hence the bandwidth of the adaptive control system is lower than the gain of the robust linear system". Also, a study to experimentally evaluate the dynamic inversion schemes is presented in [14] wherein the "backlash inverters" were found to actually degrade performance in the experiments. Besides, these inversion schemes pertain to position controlled drive systems and are not directly applicable to speed controlled systems.

Quantitative design of a class of nonlinear systems with parameter uncertainty was considered in [19]. The nonlinearities $y = N(x)$ considered are such that they can be expressed as $y = Kx + \eta(x)$ where $|\eta(x)| < M$. Several nonlinearities, such as preload, deadzone, quantization, dry friction, and backlash, are shown to belong to this class. Using this idea, a scheme to reduce the amplitude of limit cycles caused by backlash was proposed in [20].

In contrast to the number of papers published on position control in the presence of backlash, the number of papers published on the speed control is relatively few [15–18]. This lack of interest, is partially due to the fact that high precision *speed* control is not required for as many systems. A noted exception to this observation are the web handling systems where tight tension control mandates even tighter velocity control. In [16], a nonlinear controller with "soft switching" is proposed. Though improved performance

was shown on a large real life drive system, it is not clearly explained how the gains of the low-gain and high-gain controllers are computed. A gear torque compensation scheme using a PID speed controller is proposed in [15]. Though it is a novel idea, the PID gains appear to be chosen according to an *ad hoc* empirical formulae. A backlash compensation scheme using an open-loop modification of the input trajectory was proposed in [18]. The proposed velocity compensation method is most efficient only for low operating speeds and large mounting allowance between gears.

Extensive literature survey on modeling and control of industrial speed controlled drives indicates that there is a definite need for a simple model of backlash. Besides, it is of practical importance to know the achievable accuracy level in a given drive system with a known backlash. This practical consideration is not addressed in any of the existing literature. Motivated by this practical aspect, subsequent sections present a backlash model and a bound on the achievable accuracy in a given plant with a given backlash.

BACKLASH MODEL WITH COMPLIANCE

This section considers transmission systems in which backlash and compliance exist, as shown in Figures 5 and 7. Compliance in the transmission systems is considered to arise either due to the elasticity of shafts on which gears are mounted, or due to the belt in belt driven systems. The case of a compliant shaft is considered first, followed by the case of a compliant belt.

A model of backlash with a compliant shaft

To develop a simplified model, consider the schematic shown in Figure 5. In this figure, a load (J_L) is driven through a compliant shaft (k is the stiffness) and a pair of gears (radii R_1 and R_2). Usually, the motor (J_m), is mounted near the driving gear, thus the driving shaft may be assumed to be rigid.

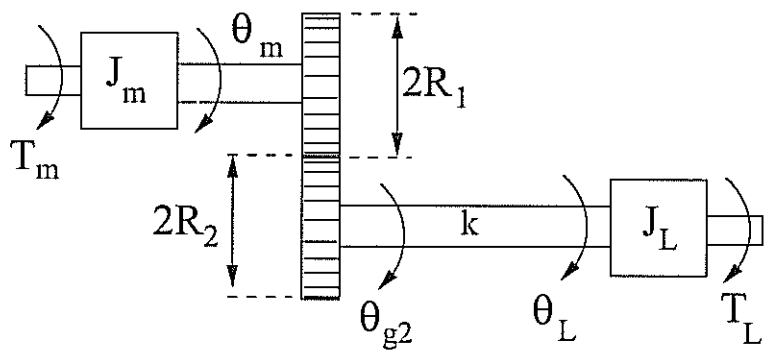

Figure 5 - Schematic of a gear drive

To avoid jamming of the gears at high speeds, the gears are mounted with a center distance slightly greater than the designed center distance. This gives rise to clearance between the mating teeth; this clearance is termed "backlash". To pictorially represent

backlash in torsional systems, at least two orthographic views are needed *viz.*, a front view as shown in Figure 5 and a side view. Also, for studying the effect of a given backlash on the output speed experimentally, one has to assemble the system shown in Figure 5 by varying the center distance between the gears. Such experimentation demands a lot of time, effort, and very precise measurement and mounting techniques. This is especially so, since the relation between the center distance and amount of backlash gap is not linear. Due to these reasons, often, the rotary system shown in Figure 5 is analyzed using a rectilinear analog as shown in Figure 6. When a rectilinear analog is used, pictorial representation as well as experimentation is considerably simplified.

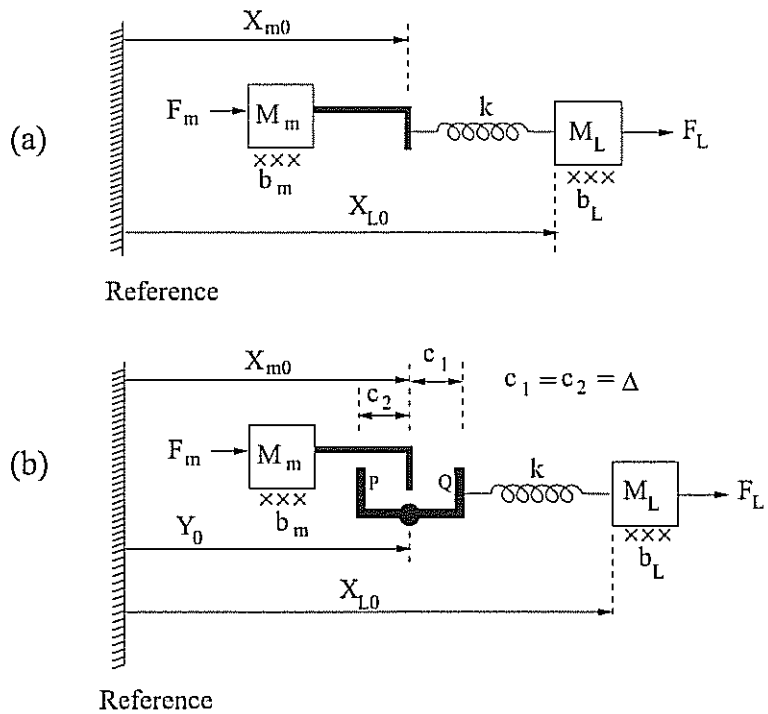

Figure 6 - Rectilinear analog: (a) without backlash, (b) with backlash

Figures 6(a) and 6(b), respectively, show a rectilinear analog of the system with and without backlash. The objective of the analysis is to study how the linearity of the system shown in Figure 6(a) gets affected by introducing backlash as shown in Figure 6(b). To obtain the equations of motion for the system shown in Figure 6(b), first conditions under which contact occurs at points P or Q need to be evaluated. Without loss of generality, consider the displacements X_{m0}, Y_0, and X_{L0} as shown in Figure 6(b).

The free length of the spring when the system is at rest is obtained as

$$L_{s0} = X_{L0} - Y_0 - \Delta. \tag{1}$$

Defining the deviations

$$\begin{aligned} x_m &= X_m - X_{m0}, \\ x_L &= X_L - X_{L0}, \\ y &= Y - Y_0, \end{aligned} \tag{2}$$

contact at point P occurs if

$$X_m = Y - \Delta, \quad \text{that is, if} \quad x_m = y - \Delta \tag{3}$$

and contact occurs at point Q if

$$X_m = Y + \Delta, \quad \text{that is, if} \quad x_m = y + \Delta. \tag{4}$$

The length of the spring at any instant of time is obtained as

$$L_s = X_L - Y - \Delta = x_L + X_{L0} - y - Y_0 - \Delta = (x_L - y) + L_{s0}. \tag{5}$$

Thus, when contact occurs at point P, the length of the spring may be obtained from equations (3) and (5) as

$$L_P = (x_L - x_m - \Delta) + L_{s0}. \tag{6}$$

If loss of contact at point P were to occur, it must be either due to mass M_m moving to the right, that is due to increase in x_m, or due to mass M_L moving to the left, that is due to decrease in x_L. In either case, loss of contact at P is occurring due to decrease in $(x_L - x_m)$ and thus, due to decrease in $(x_L - x_m - \Delta)$. Since the spring tries to regain its original length soon after contact is lost, we say that, L_P keeps on changing till either its value is equal to L_{s0} or a contact is established, whichever occurs first. From (6), we see that if the value of L_P tends to change in the direction of L_{s0} and $(x_L - x_m - \Delta)$ is decreasing soon after loss of contact, we see that, to begin with $(x_L - x_m - \Delta)$ must be greater than or equal to zero. Thus,

$$(x_L - x_m - \Delta) \geq 0 \tag{7}$$

is the condition for sustained contact at P and $(x_L - x_m - \Delta)$ is the change in the length of the spring. Similarly, we see that the condition for contact at point Q is

$$(x_L - x_m + \Delta) \leq 0 \tag{8}$$

and $(x_L - x_m + \Delta)$ is the change in the length of the spring.

From equations (7) and (8), we see that, as long as there is no contact,

$$-\Delta < (x_L - x_m) < \Delta. \tag{9}$$

With the contact conditions given by (7), (8), and (9), the kinetic energy and the potential energy of the system shown in Figure 6(b) may be written as

$$\begin{aligned} K(\dot{x}_m, \dot{x}_L) &= \frac{1}{2}[M_m \dot{x}_m^2 + M_L \dot{x}_L^2] \\ V(x_m, x_L) &= \begin{cases} \frac{1}{2}k(x_L - x_m - \Delta)^2 & \text{if (7) holds} \\ \frac{1}{2}k(x_L - x_m + \Delta)^2 & \text{if (8) holds} \\ 0 & \text{if (9) holds} \end{cases} \end{aligned} \tag{10}$$

With the kinetic energy and potential energy defined in (10), the Euler-Lagrange dynamics for the system shown in Figure 6(b), ignoring the inertias of the spring and the shaft, may be written as

$$\begin{aligned} M_m\ddot{x}_m + b_m\dot{x}_m + \psi(x_m, x_L) &= F_m, \\ M_L\ddot{x}_L + b_L\dot{x}_L - \psi(x_m, x_L) &= F_L, \end{aligned} \tag{11}$$

where

$$\psi(x_m, x_L) = \begin{cases} k(x_m - x_L + \Delta) & \text{if (7) holds,} \\ k(x_m - x_L - \Delta) & \text{if (8) holds,} \\ 0 & \text{if (9) holds.} \end{cases} \tag{12}$$

Effect of belt compliance and backlash in gears

This section considers the effect of backlash on the output speed of the transmission system which has belt-pulley arrangement as shown in Figure 7. Since a pair of mating spur gears rotate in opposite directions, a sign convention is needed to keep track of the angular displacements. The sign convention followed here is that, looking from the load side (that is, from the right hand side of Figure 7), θ is considered to be positive in counter-clockwise direction and θ_L is considered to be positive in clockwise direction.

Also, reference for angular displacements is taken to be $\theta_m = \theta = \theta_L = 0$ and hence, the deviations in the angular displacements and their absolute values are the same. Further let the free-length of the tight side of the belt in Figure 7 be L_0.

At any instant, the length of the tight side of the belt may be obtained as

$$L = L_0 + (R_2\theta - R_1\theta_m). \tag{13}$$

A condition for contact at point P is determined by considering the length of the tight side of the belt when contact does exist at point P. First, notice that, for contact at point P,

$$R_{g1}\theta = R_{g2}\theta_L + \Delta \quad \Rightarrow \theta = \frac{1}{R_{g1}}[R_{g2}\theta_L + \Delta] \tag{14}$$

which indicates that a point on the pitch circle of gear 1 has to travel an extra distance of Δ for contact to be established. Thus, the length of the tight side of the belt during sustained contact at point P may be written as

$$L_P = L_0 + \frac{R_2}{R_{g1}}[R_{g2}\theta_L + \Delta] - R_1\theta_m \triangleq \alpha_1\theta_L - R_1\theta_m + \alpha_2\Delta + L_0 \tag{15}$$

where $\alpha_1 \triangleq R_2G_R$, $\alpha_2 \triangleq R_2/R_{g1}$, and $G_R = R_{g2}/R_{g1}$. Contact at point P will be lost either when θ decreases or when θ_L increases. In either case, $(\alpha_1\theta_L - R_1\theta_m + \alpha_2\Delta)$ increases. Therefore, upon loss of contact, $L_P \rightarrow L_0$. Coupled with this fact, $(\alpha_1\theta_L - R_1\theta_m + \alpha_2\Delta)$ increases when contact is lost at point P means that to begin with

$$(\alpha_1\theta_L - R_1\theta_m + \alpha_2\Delta) \leq 0. \tag{16}$$

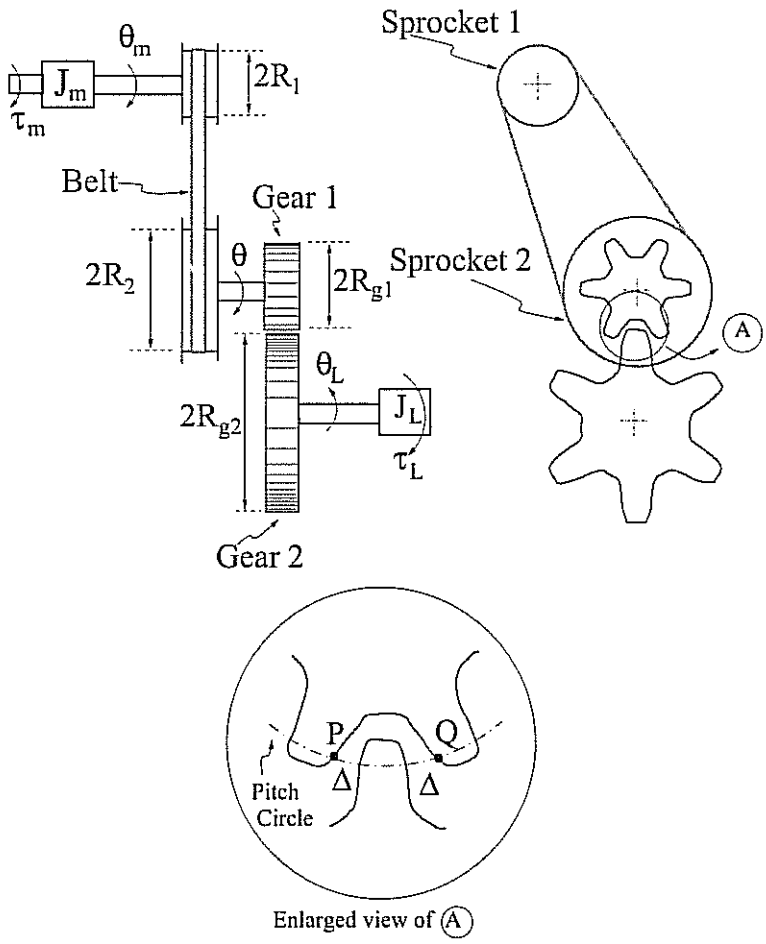

Figure 7 - Schematic of a belt-pulley transmission system.

Thus, (16) gives a condition for contact at point P. The quantity on the left hand side of inequality (16) is the change in the length of the tight side of the belt. Similarly, condition for contact at point Q may be written as

$$(\alpha_1\theta_L - R_1\theta_m - \alpha_2\Delta) \geq 0. \tag{17}$$

The quantity on the left hand side of inequality in (17) is change in the length of the tight side of the belt. From equations (16) and (17), when there is no contact,

$$-\alpha_2\Delta < \alpha_1\theta_L - R_1\theta_m < \alpha_2\Delta. \tag{18}$$

Thus, the kinetic energy and the potential energy of the system shown in Figure 7 may be

written as

$$K(\dot{x}_m, \dot{x}_L) = \frac{1}{2}[J_m\dot{\theta}_m^2 + J_L\dot{\theta}_L^2]$$

$$V(x_m, x_L) = \begin{cases} \frac{1}{2}K_b(\alpha_1\theta_L - R_1\theta_m + \alpha_2\Delta)^2 & \text{if (16) holds} \\ \frac{1}{2}K_b(\alpha_1\theta_L - R_1\theta_m - \alpha_2\Delta))^2 & \text{if (17) holds} \\ 0 & \text{if (18) holds.} \end{cases} \tag{19}$$

Using the kinetic energy and the potential energy given in (19), the Euler-Lagrange dynamics of the system shown in Figure 7, ignoring the inertias of the pulleys and the gears, may be written as:

$$J_m\ddot{\theta}_m + b_m\dot{\theta}_m + R_1\psi(\theta_m, \theta_L) = \tau_m \tag{20a}$$

$$J_L\ddot{\theta}_L + b_L\dot{\theta}_L - \alpha_1\psi(\theta_m, \theta_L) = \tau_L \tag{20b}$$

where

$$\psi(\theta_m, \theta_L) = K_b \begin{cases} (R_1\theta_m - \alpha_1\theta_L - \alpha_2\Delta) & \text{if (16) holds} \\ (R_1\theta_m - \alpha_1\theta_L + \alpha_2\Delta) & \text{if (17) holds} \\ 0 & \text{if (18) holds.} \end{cases} \tag{21}$$

ERROR BOUNDS IN THE PRESENCE OF BACKLASH

This section presents a bound on the error due to the presence of backlash. The idea behind the approach is to consider backlash-free system and see how the presence of backlash affects the dynamics. First, the case of compliant shaft and backlash, as shown in Figure 5 is considered, followed by the case of compliant belt and backlash, as shown in Figure 7.

Bound on error due to backlash and a compliant shaft

To arrive at a bound on error due to the presence of backlash, consider the situation without backlash, shown in Figure 6(a). When the system is at rest, the displacements of the masses are X_{m0} and X_{L0} from a fixed reference as shown in Figure 6(a) and the free length of the spring is

$$L_{s0} = X_{L0} - X_{m0}. \tag{22}$$

When the system is in motion, let X_L and X_m be the displacements of the masses from the fixed reference. Defining the deviations

$$\begin{aligned} x_m &= X_m - X_{m0}, \\ x_L &= X_L - X_{L0}, \end{aligned} \tag{23}$$

the length of the spring at any instant of time may be written as

$$L_s = X_L - X_m = x_L + X_{L0} - x_m - X_{m0} = (x_L - x_m) + L_{s0}. \tag{24}$$

Thus, the change in the length of the spring is $L_s - L_{s0} = x_L - x_m$ and kinetic energy and potential energy of the system may be written as

$$\begin{aligned} K(\dot{x}_m,\, \dot{x}_L) &= \frac{1}{2}[M_m\dot{x}_m^2 + M_L\dot{x}_L^2], \\ V(x_m,x_L) &= \frac{1}{2}k[x_m^2 + x_L^2]. \end{aligned} \tag{25}$$

Using the well-known Euler-Lagrange equations of motion, the dynamics of the system shown in Figure 6(a) may be obtained as

$$\begin{aligned} M_m\ddot{x}_m + b_m\dot{x}_m + k(x_m - x_L) &= F_m, \\ M_L\ddot{x}_L + b_L\dot{x}_L - k(x_m - x_L) &= F_L. \end{aligned} \tag{26}$$

Upon rearranging the terms in equations (11) and (12), the dynamics of the system shown in Figure 6(b) may be written as

$$\begin{aligned} M_m\ddot{x}_m + b_m\dot{x}_m + k(x_m - x_L) - \phi(x_m,x_L) &= F_m, \\ M_L\ddot{x}_L + b_L\dot{x}_L - k(x_m - x_L) + \phi(x_m,x_L) &= F_L, \end{aligned} \tag{27}$$

where

$$\phi(x_m,x_L) = \begin{cases} -k\Delta & \text{if (7) holds,} \\ k\Delta & \text{if (8) holds,} \\ k(x_m - x_L) & \text{if (9) holds.} \end{cases} \tag{28}$$

Notice that equations (26) and (27) are identical except for the extra term, $\phi(x_m,x_L)$, present in (27). And this extra term, because of the condition in (9), is bounded by $|\phi(x_m,x_L)| \leq k\Delta$ for all $x_m,\ x_L \in \mathbb{R}$. Defining the state-variables $z_{m1} = x_m$, $z_{m2} = v_m = \dot{x}_m$, $z_{L1} = x_L$, $z_{L2} = v_L = \dot{x}_L$, and $z = [z_{m1}, z_{m2}, z_{L1}, z_{L2}]^\top$, a state space representation of the system shown in Figure 6(b) is obtained as

$$\begin{aligned} \dot{z} &= A_p z + B_p F_m + C_p F_L + \beta D_p(x_m,x_L) \\ y &= L_p z \end{aligned} \tag{29}$$

where

$$\begin{aligned} A_p &= \begin{bmatrix} 0 & 1 & 0 & 0 \\ -\frac{k}{M_m} & -\frac{b_m}{M_m} & \frac{k}{M_m} & 0 \\ 0 & 0 & 0 & 1 \\ \frac{k}{M_L} & 0 & -\frac{k}{M_L} & -\frac{b_L}{M_L} \end{bmatrix}, \quad B_p = \begin{bmatrix} 0 \\ \frac{1}{M_m} \\ 0 \\ 0 \end{bmatrix}, C_p = \begin{bmatrix} 0 \\ 0 \\ 0 \\ \frac{1}{M_L} \end{bmatrix}, \\ D_p(x_m,x_L) &= \begin{bmatrix} 0 \\ \frac{\phi(x_m,x_L)}{M_m} \\ 0 \\ -\frac{\phi(x_m,x_L)}{M_L} \end{bmatrix}, \quad L_p = \begin{bmatrix} 0 & 1 & 0 & 0 \\ 0 & 0 & 0 & 1 \end{bmatrix} \triangleq \begin{bmatrix} L_{p1} \\ L_{p2} \end{bmatrix} \end{aligned} \tag{30}$$

and β is zero if the backlash gap is zero and unity otherwise. Thus, with $\beta = 0$, (29) is a state space representation of the system shown in Figure 6(a) and with $\beta = 1$, (29) is a state space representation of the system shown in Figure 6(b). Equation (29) represents a

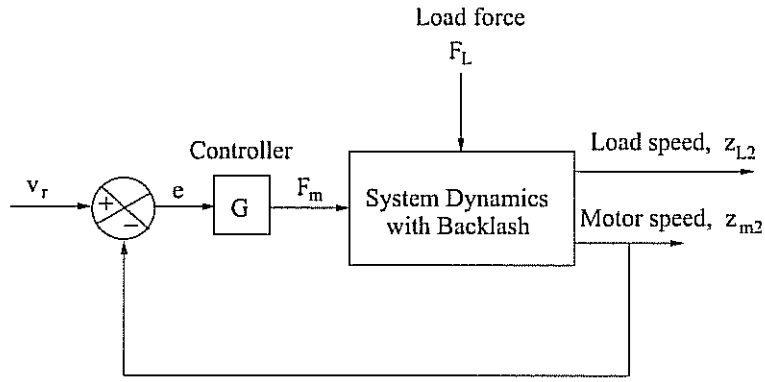

Figure 8 - Block diagram of a controller for system with backlash

system with two inputs (the actuating force, F_m and load force, F_L) and two outputs (the motor speed, z_{m2} and the load speed, z_{L2}) as shown in Figure 8.

In the control scheme shown in Figure 8, the controller, G, uses feedback from the motor-side (z_{m2}). If the load velocity is used as feedback, the controller may keep on accelerating/decelerating the motor during the no-contact period since the motor has no "control" over the load during the no-contact period. This might have been the reason for specific lack of interest in using the load side feedback, as noted in [9, Section 3].

Suppose the controller, G, has the state-space representation

$$\begin{aligned} \dot{x}_c &= A_c x_c + B_c e, \\ F_m &= C_c x_c + D_c e. \end{aligned} \tag{31}$$

Then the state-space representation for the closed-loop system shown in Figure 8 may be obtained as

$$\begin{aligned} \dot{z}_{cl} &= A_{cl} z_{cl} + C_{cl} F_L + W v_r + D_{cl}(x_m, x_L) \\ z^b_{L2} &= L_c z_{cl} \end{aligned} \tag{32}$$

where $z_{cl} = [z^\top \;\; x_c^\top]^\top$, $W = [D_c^\top B_p^\top \;\; B_c^\top]^\top$, $L_c = [0 \;\; 0 \;\; 0 \;\; 1 \;\; \mathbf{0}]$, and

$$A_{cl} = \begin{bmatrix} (A_p - B_p D_c L_{p1}) & B_p C_c \\ -B_c L_{p1} & A_c \end{bmatrix}, \quad C_{cl} = \begin{bmatrix} C_p \\ \mathbf{0} \end{bmatrix}, \quad D_{cl}(x_m, x_L) = \begin{bmatrix} D_p(x_m, x_L) \\ \mathbf{0} \end{bmatrix}. \tag{33}$$

The superscript in z^b_{L2} indicates the output in the presence of backlash. If the backlash were to be absent, $\beta = 0$ and the state-space representation of the closed-loop system may be written as

$$\begin{aligned} \dot{v}_{cl} &= A_{cl} v_{cl} + C_{cl} F_L + W v_r \\ z^0_{L2} &= L_c v_{cl} \end{aligned} \tag{34}$$

where the matrices A_{cl}, C_{cl}, W are given in (33) and z^0_{L2} is the output in the absence of backlash. Equations (32) and (34) are similar except for the last term in the state equation in (32) and the deviation $|z^b_{L2} - z^0_{L2}| = |L_c(z_{cl} - v_{cl})|$ represents the effect of backlash.

For a given reference velocity v_r, and the disturbance force F_L, solution of the state equation in (34) is obtained as

$$v_{cl}(t) = e^{A_{cl}t}v_{cl}^0 + \int_0^t e^{A_{cl}(t-\tau)}[F_L(\tau) + Wv_r(\tau)]d\tau \triangleq \phi(v_r, F_L, t). \tag{35}$$

where $v_{cl}(0) = v_{cl}^0$ is the initial condition. Then, taking the initial condition to be $z_{cl}(0) = z_{cl}^0 = v_{cl}^0$, the solution of the state equation in (32) may be written as

$$z_{cl}(t) = \phi(v_r, F_L, t) + \int_0^t e^{A_{cl}(t-\tau)}D_{cl}(x_m(\tau),\, x_L(\tau))d\tau \tag{36}$$

Thus, the deviation in state variable due to the effect of backlash may be written as

$$\begin{aligned} \|z_{cl} - v_{cl}\|(t) &= \left\| \int_0^t e^{A_{cl}(t-\tau)}D_{cl}(x_m(\tau),\, x_L(\tau))d\tau \right\| \\ &\leq k\Delta \left\| \int_0^t e^{A_{cl}(t-\tau)}D_1 d\tau \right\| \triangleq \delta_b \end{aligned} \tag{37}$$

where $D_1 = [0 \;\; 1/M_m \;\; 0 \;\; -1/M_L \;\; 0]^\top$.

Bound on error due to backlash and belt compliance

This section considers the schematic of the transmission system shown in Figure 7 and presents a bound on the error due to the presence of backlash.

Defining the state-variables $z_{m1} = \theta_m$, $z_{m2} = \omega_m = \dot{\theta}_m$, $z_{L1} = \theta_L$, $z_{L2} = \omega_L = \dot{\theta}_L$, and $z = [z_{m1}, z_{m2}, z_{L1}, z_{L2}]^\top$, and using the equations (20), (21), a state-space representation of the system shown in Figure 7 is obtained as[1]

$$\begin{aligned} \dot{z} &= A_p z + B_p \tau_m + C_p \tau_L + \beta D_p(\theta_m, \theta_L) \\ y &= L_p z \end{aligned} \tag{38}$$

where

$$\begin{aligned} A_p &= \begin{bmatrix} 0 & 1 & 0 & 0 \\ -\frac{K_b R_1^2}{J_m} & -\frac{b_m}{J_m} & \frac{K_b R_1 \alpha_1}{J_m} & 0 \\ 0 & 0 & 0 & 1 \\ \frac{K_b \alpha_1 R_1}{J_L} & 0 & -\frac{K_b \alpha_1^2}{J_L} & -\frac{b_L}{J_L} \end{bmatrix}, \quad B_p = \begin{bmatrix} 0 \\ \frac{1}{J_m} \\ 0 \\ 0 \end{bmatrix}, C_p = \begin{bmatrix} 0 \\ 0 \\ 0 \\ \frac{1}{J_L} \end{bmatrix}, \\ D_p(x_m, x_L) &= \begin{bmatrix} 0 \\ -\frac{R_1 \phi(\theta_m, \theta_L)}{J_m} \\ 0 \\ \frac{\alpha_1 \phi(\theta_L, \theta_L)}{J_L} \end{bmatrix}, \quad L_p = \begin{bmatrix} 0 & 1 & 0 & 0 \\ 0 & 0 & 0 & 1 \end{bmatrix} \triangleq \begin{bmatrix} L_{p1} \\ L_{p2} \end{bmatrix} \end{aligned} \tag{39}$$

[1]The same symbols A_p, B_p etc. are used here and in equation (30) to highlight the fact that the dynamic models for the rectilinear analog shown in Figure 6 and the system shown in Figure 7 are "analogous" to each other.

and β is zero if the backlash gap is zero and unity otherwise and $\phi(\theta_m, \theta_L)$ is defined as

$$\phi(\theta_m, \theta_L) = K_b \begin{cases} -\alpha_2 \Delta & \text{if (16) holds} \\ \alpha_2 \Delta & \text{if (17) holds} \\ (\alpha_1 \theta_L - R_1 \theta_m) & \text{if (18) holds.} \end{cases} \tag{40}$$

Equation (38) represents a system with two inputs (the actuating force, τ_m and load force, τ_L) and two outputs (the motor speed, z_{m2} and the load speed, z_{L2}) as shown in Figure 8. Consequently, a bound, as given in (37) may be obtained.

Comparing the equations (28) and (40), we see that an additional term $\alpha_2 = R_2/R_{g1}$ multiplies the backlash width Δ in the case of analysis of the effect of belt and backlash. Due to this term, the bound given in (37) is modified to

$$\begin{aligned} \|z_{cl} - v_{cl}\|(t) &= \left\| \int_0^t e^{A_{cl}(t-\tau)} D_{cl}(x_m(\tau),\, x_L(\tau)) d\tau \right\| \\ &\leq K_b \alpha_2 \Delta \left\| \int_0^t e^{A_{cl}(t-\tau)} D_1 d\tau \right\| \triangleq \delta_b \end{aligned} \tag{41}$$

for the case of belt compliance. In equation (41), $D_1 = [0,\ -R_1/J_m,\ 0,\ \alpha_1/J_L,\ 0]^\top$. If α_2 is small, the bound δ_b is also small and so it is advantageous to have $R_2/R_{g1} \ll 1$.

EXPERIMENTS

This section presents experiments conducted to verify the error bound due to backlash, given in (37). The experimental setup, shown in Figure 9, consists of two masses mounted on carriages which are free to slide. A spring is used to represent the compliance k shown in Figure 6. That is the system shown in Figure 6 is realized as masses 1 and 2 connected by a spring so that $M_m = M_1$ and $M_L = M_2$.

Position of each of the masses is measured by a high resolution encoder. Nominal values of the masses are M_1=2.28 kg and M_2=2.55 kg. Nominal stiffness of the spring is k=200 N/m. The damping present at masses, as estimated by a preliminary identification procedure, are $b_m = b_L$ =0.05 N-s/m.

Backlash is introduced into the system shown in Figure 9 between the spring and mass 1. Figure 10 shows a close-up view of the system showing the backlash gap. Through a simple screw-and-locking-nut arrangement, the length of the backlash gap can be adjusted accurately.

A Proportional-Integral (PI) controller, using velocity of mass 1 as feedback signal, is implemented to impart a prescribed velocity to mass 1. Positions and velocities of the masses 1 and 2 are acquired firstly without backlash present in the system and then with a known backlash. From each set of experiments, the difference between the load velocity (velocity of mass 2) with backlash and load velocity without backlash is computed using the experimental data. This difference is then compared with the bound computed using (37). Figures 11, 12, and 13 show the results of experiments. The solid line in Figure 11 shows the deviation in the load velocity due to presence of backlash obtained from experimental data and the dashed horizontal line shows the bound on the deviation as

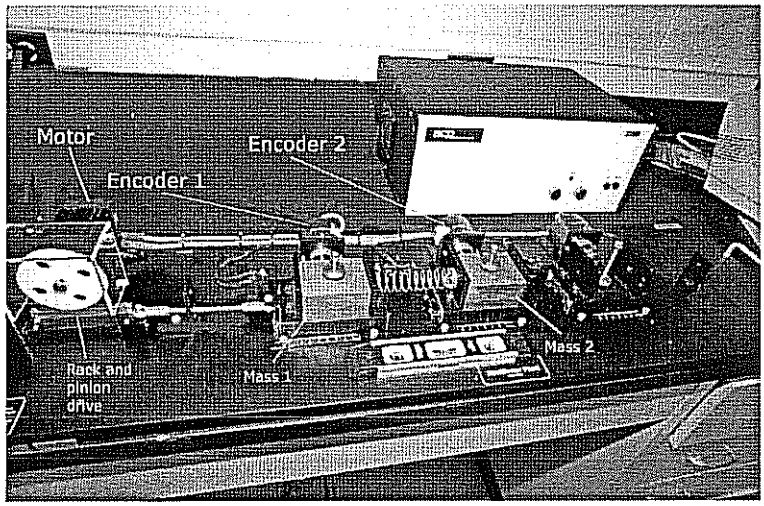

Figure 9 - ECP Rectilinear System

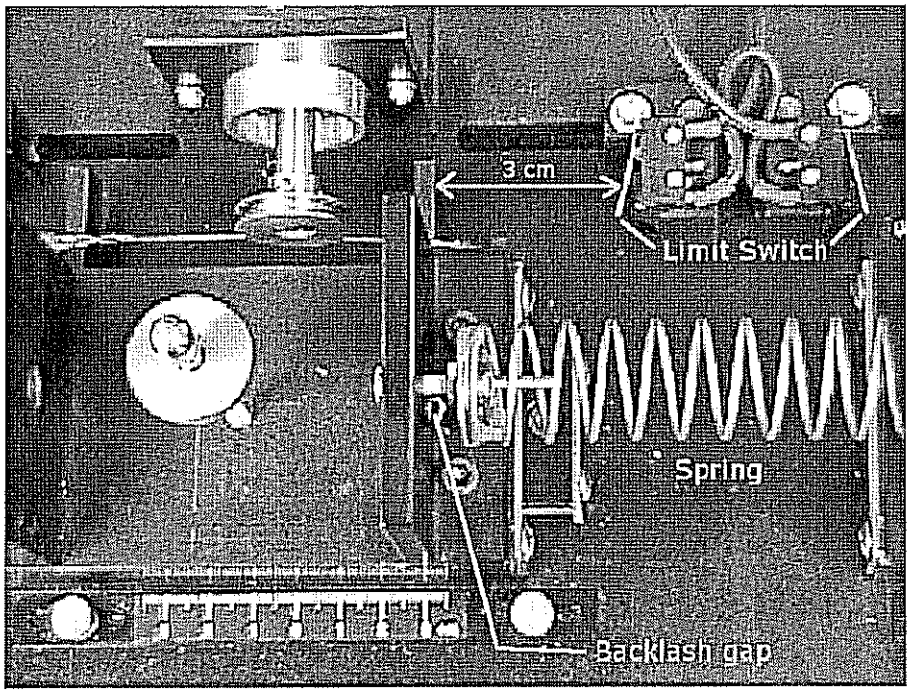

Figure 10 - Backlash gap in experiments.

evaluated from (37) using a backlash gap of 1.55 mm. It is noticed that the experimentally evaluated deviation is within the bound.

Similarly, Figures 12 and 13 show the results with backlash gaps of 3.56 mm and 5.38 mm, respectively. These figures show that the deviation due to presence of backlash, as evaluated from experiments is within the bound obtained using (37).

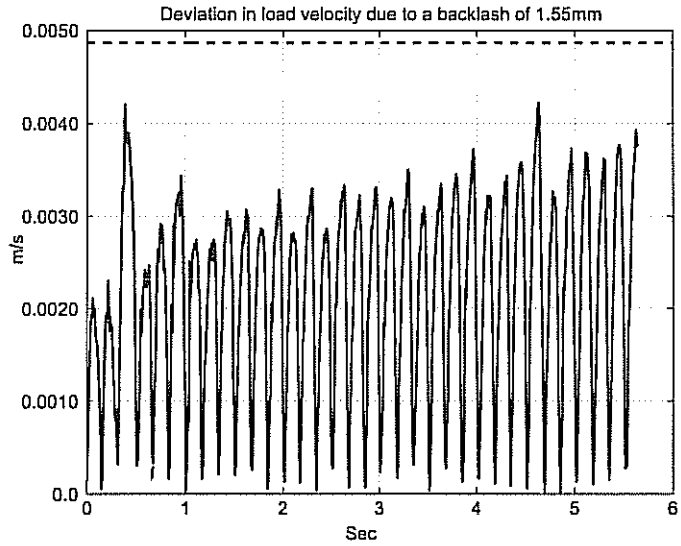

Figure 11 - Closed-loop experiment with backlash of 1.55 mm

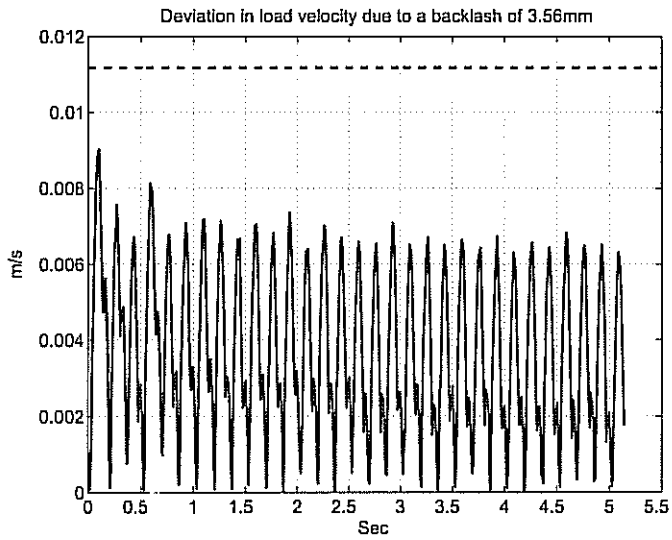

Figure 12 - Closed-loop experiment with backlash of 3.56 mm

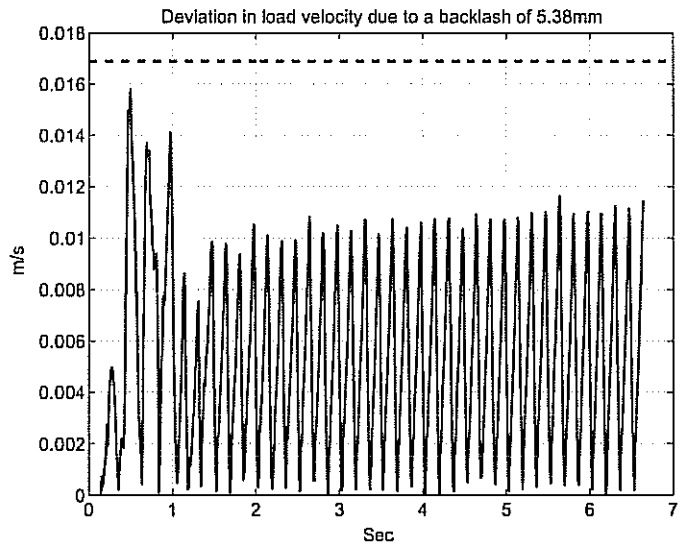

Figure 13 - Closed-loop experiment with backlash of 5.38 mm

SUMMARY AND FUTURE WORK

A model for backlash to include the dynamics of the driven member during the period of loss of contact and the effect of disturbing forces on the load is presented. Using the model, an upper bound on the achievable accuracy in a given system using a given controller is obtained. Experiments conducted on a prototype system agree with the theoretically estimated upper bound.

In a typical web handling system, the "load" shown in Figure 5 comprises of the unwind/winder shaft and the roll mounted on it. Any variations in the web velocity due to the presence of compliance and backlash in the transmission system directly affect the web tension, which is an important controlled variable. In the context of web handling systems, the following two aspects may be considered as future work.

- The effect of web velocity variations due to the presence of compliance/backlash on the controlled web tension is an important aspect which needs to be further investigated.

- It is of importance to know the permissible values of compliance and backlash to yield a given accuracy in web velocity and web tension. Deriving these permissible values of compliance and backlash will prove to be an important extension to the present work.

REFERENCES

[1] D. Schulkind, "Accuracy requirements of nonlinear compensation for backlash," *IRE Transactions on Automatic Control*, vol. 5, pp. 79–85, June 1960.

[2] J. Marstrander and R. Lueg, "Limit cycle determination for instrument servomechanism with backlash," *IEEE Transactions on Automatic Control*, vol. 14, pp. 756–757, December 1969.

[3] H. Maeda, M. Ikeda, and S. Kodama, "Stability criterion for a feedback system with backlash," *IEEE Transactions on Automatic Control*, vol. 15, pp. 703–705, December 1970.

[4] R. Ringland, "Sinusoidal input describing function for hysteresis followed by elementary backlash," *IEEE Transactions on Automatic Control*, vol. 21, pp. 285–288, April 1976.

[5] S. Dubowsky and F. Freudenstein, "Dynamic analysis of mechanical systems with clearance: Part 1: Formulation of dynamic model," *ASME Journal of Engineering for Industry*, vol. 93, pp. 305–309, February 1971.

[6] S. Dubowsky and F. Freudenstein, "Dynamic analysis of mechanical systems with clearance: Part 2: Dynamic response," *ASME Journal of Engineering for Industry*, vol. 93, pp. 310–316, February 1971.

[7] R. Azar and F. Crossley, "Digital simulation of impact phenomenon in spur gear systems," *ASME Journal of Engineering for Industry*, vol. 99, pp. 792–79, 1977.

[8] D. Yang and Z. Sun, "A rotary model for spur gear dynamic," *ASME Journal of Mechanisms, Transmissions and Automation in Design*, vol. 107, pp. 529–535, December 1998.

[9] M. Nordin and P.-O. Gutman, "Controlling mechanical systems with backlash - a survey," *Automatica*, vol. 38, pp. 1633–1649, 2002.

[10] J.-G. Kim and D. H. Chyung, "Digital controller for systems containing a backlash," in *Proceedings of the 32nd Conference on Decision and Control*, pp. 323–324, December 1993.

[11] G. Tao and P. V. Kokotovic, "Adaptive control of systems with backlash," *Automatica*, vol. 29, no. 2, pp. 323–335, 1993.

[12] J. Campos, R. R. Selmic, and F. L. Lewis., "Backlash compensation in nonlinear systems by dynamic inversion using neural networks: Continuous and discrete time approaches." downloaded from website, December 1999. http://arri.uta.edu/acs/jcampos/research/backctdt.pdf.

[13] D. Seidl, S.-L. Lam, J. Putman, and R. Lorenz, "Neural network compensation of gear backlash hysteresis in position-controlled mechanisms," *IEEE Transactions on Industry Applications*, vol. 31, no. 6, pp. 1475–1483, 1995.

[14] S. R. Dean, B. W. surgenor, and H. N. Iordanou, "Experimental evaluation of a backlash inverter as applied to a servomotor with gear train," in *Proceedings of the 4th IEEE Conference on Control Applications*, pp. 580–585, September 1995.

[15] M. Odai and Y. Hori, "Speed control of two-inertia system with gear backlash based on gear torque compensation," *Electrical Engineering in Japan*, vol. 134, no. 2, pp. 36–43, 2001. Translated from Denki Gakkai Ronbushi vol. 120-D, No. 1, January 2000, pp. 5–10.

[16] M. Nordin and P.-O. Gutman, "Non-linear speed control of elastic systems with backlash," in *Proceedings of the 39th IEEE Conference on Decision and Control*, pp. 4060–4065, December 2000.

[17] M. L. Corradini and G. Orlando, "Robust stabilization of nonlinear uncertain plants with backlash or deadzone in the actuator," *IEEE Transactions on Control Systems Technology*, vol. 10, pp. 158–166, January 2002.

[18] M. Warnecke and M. Jouaneh, "Backlash compensation in gear trains by means of open-loop modification of the input trajectory," *ASME Journal of Mechanical Design*, vol. 125, pp. 620–624, September 2003.

[19] S. Oldak, C. Baril, and P. Gutman, "Quantitative design of a class of nonlinear systems with parameter uncertainity," *International Journal of Robust and Nonlinear Control*, vol. 4, pp. 101–117, 1994.

[20] R. Boneh and O. Yaniv, "Reduction of limit cycle amplitude in the presence of backlash," *ASME Journal of Dynamic Systems, Measurement, and Control*, vol. 121, pp. 278–284, June 1999.